

Four-neutrino Oscillations at SNO

C. Peña-Garay^{a*}

^aInst. de Física Corpuscular, C.S.I.C. - Univ. de València, Spain

We discuss the potential of the Sudbury Neutrino Observatory (SNO) to constraint the four-neutrino mixing schemes favoured by the results of all neutrino oscillations experiments. Our results show that some information on the value of $\cos^2(\vartheta_{23}) \cos^2(\vartheta_{24})$ can be obtained by the first SNO measurement of the CC ratio, while considerable improvement on the knowledge of this mixing will be achievable after the measurement of the NC/CC ratio.

1. Introduction

The Sudbury Neutrino Observatory is a second generation water Cerenkov detector using 1000 tonnes of heavy water, D_2O , as detection medium. SNO was designed to address the problem of the deficit of solar neutrinos by having sensitivity to all flavours of neutrinos and not just to ν_e , allowing for a model independent test of the oscillation explanation of the observed deficit. Such sensitivity can be achievable because energetic neutrinos can interact in the D_2O of SNO via three different reactions. Electron neutrinos may interact via the Charged Current (CC) reaction. All non-sterile neutrinos may also interact via Neutral Current (NC) and via Elastic Scattering (ES) (smaller cross section).

The main objective of SNO is to measure the ratio of NC/CC events. In its first year of operation SNO is concentrating on the measurement of the CC reaction rate while in a following phase, after the addition of $MgCl_2$ salt to enhance the NC signal, it will also perform a precise measurement of the NC rate. It is clear that a cross-section-normalized and acceptance-corrected ratio higher than 1 would strongly indicate the oscillation of ν_e into ν_μ and/or ν_τ . On the other hand a deficit on both CC and NC leading to a normalized NC/CC ratio 1, can only be made compatible with the oscillation hypothesis if ν_e oscillates in to a sterile neutrino.

Most of the studies of the potential of SNO have been performed in the framework of oscillations between two neutrino states where ν_e oscillates into either an active, $\nu_e \rightarrow \nu_a$, or a sterile, $\nu_e \rightarrow \nu_s$, neutrino channel. On the other hand, once the possibility of a sterile neutrino is considered, these two scenarios are only limiting cases of the most general mixing structure [1,2] which permits simultaneous $\nu_e \rightarrow \nu_s$ and $\nu_e \rightarrow \nu_a$ oscillations. We consider those four-neutrino schemes favoured by considering together with the solar neutrino data, the results of the two additional evidences pointing out towards the existence of neutrino masses and mixing: the atmospheric neutrino data and the LSND results. We concentrate on two SNO measurements: the first expected result on the CC ratio and the expected to be most sensitive, the ratio of NC/CC. The measurement of other observables, such as the recoil energy spectrum of the CC events and the zenith angular dependence can provide important information to distinguish between the different allowed regions for ν_e -active oscillations but they are not expected to be very sensitive as discriminatory between the active and sterile oscillations.

2. Two-Neutrino Mixing: Predictions for SNO

The results presented in this section have been obtained for the oscillation parameters in the presently allowed regions to the solar neutrino problem in the two-neutrino schemes. The results of the global fit to the data (Ref. [3]) include (i) the SK data after 1117 days of operation

*Talk presented at EURESCO Conference on Frontiers in Particle Astrophysics and Cosmology, San Feliu de Guixols, Spain. Based on M. C. Gonzalez-Garcia and C. Peña-Garay, hep-ph/0011245.

(total number of events and day and night energy spectra), (ii) Gallex, GNO and SAGE data, (iii) the Homestake data. We used the 90% and 99% CL regions found from the global minimum. The fit includes the latest standard solar model fluxes, BP00 model [4]. For details on the statistical analysis applied to the different observable we refer to Ref. [5].

The total number of events in the CC reaction at SNO is calculated with the νd CC cross section computed from the corresponding differential cross sections [6] folded with the finite energy resolution function of the detector and integrated over the electron recoil energy. For definiteness, we adopted the most optimistic total energy threshold $E_{th} = 5$ MeV. The total number of events in the NC reaction at SNO is obtained using the νd NC cross section from [6].

In order to cancel out all energy independent efficiencies and normalizations we will use the ratio $R_{CC}^{th} = \frac{N_{CC}^{th}}{N_{CC}^{SSM}} \equiv [CC]$ where N_{CC}^{SSM} is the predicted number of events in the case of no oscillations. The equivalent expression for the NC ratio $R_{NC}^{th} = \frac{N_{NC}^{th}}{N_{NC}^{SSM}} \equiv [NC]$ Out of those ratios one can compute the double ratio $\frac{R_{NC}^{th}}{R_{CC}^{th}} \equiv [NC]/[CC]$ for which the largest sources of uncertainties cancel out [7]. As it was shown in Ref. [6], the ratio between the NC and CC reaction cross sections is extremely stable against any variations of the inputs of the calculations. The expected total uncertainties for the [CC] ratio and the [NC]/[CC] ratio are 6.7 % and 3.6 % respectively assuming 5000 CC events and 1219 NC events [7].

In Fig. 1 we show the predicted [CC] and [NC]/[CC] ratios for the allowed regions in the two flavour analysis. The dots correspond to the local best fit points and the error bars show the range of predictions for the points inside the 90 and 99 %CL allowed regions. The mapping of the regions onto these bars can be easily understood from the behaviour of the probability for the different solutions:

(a) For oscillations into active neutrinos the [NC]/[CC] ratio is simply the inverse of the [CC] prediction. Therefore: in the SMA region smaller mixing angles are mapped onto higher (lower) val-

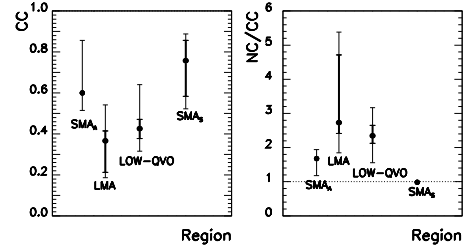


Figure 1. [CC] and [NC]/[CC] predictions at SNO for the allowed regions in the two-neutrino mixing scenarios obtained from the global analysis of solar neutrino data at 90 % and 99 %CL.

ues of [CC] ([NC]/[CC]) ratio. One may notice that the prediction for the [CC] rate for the global best fit point (0.60) is larger than the measured rate at Super-Kamiokande. This is due to the nearly flat spectrum at Super-Kamiokande which implies that the best fit point in the global analysis corresponds to a smaller mixing angle than the best fit point for the analysis of rates only; in the LMA region, the lower Δm^2 and θ values are mapped onto higher (lower) [NC]/[CC] ([CC]) ratios and viceversa; in the LOW region the higher (lower) [NC]/[CC] ([CC]) ratio occurs for smaller θ and higher Δm^2 .

(b) For the sterile case, the best fit point in SMA occurs at lower Δm^2 than in the active case and this produces a higher prediction for the [CC] ratio (0.76). The [NC]/[CC] ratio takes an almost constant value very close to one (0.98 in the best fit point), since both numerator and denominator are proportional to $\langle P_{\nu_e \rightarrow \nu_e} \rangle$. It is smaller than one because for the SMA solution the probability increases with energy in the range of detection at SNO and the threshold for the NC reaction is below the one for the CC one.

What we see from these results is that while the data on [CC] can give a hint towards large or small mixing solutions, it will be hard to distinguish active from sterile oscillations on the only bases of this measurement. This is not the case for the [NC]/[CC] ratio where both scenarios appear nicely separated. It is not hard to foresee from these results that from the [NC]/[CC] measurement SNO will be able to constraint the

additional mixings in the four-neutrino scenario which describe the admixture of active and sterile oscillations. This is the main point in this paper.

3. Allowed Four-neutrino Mixing Parameters

Together with the results from the solar neutrino experiments we have two more evidences pointing out towards the existence of neutrino masses and mixing: the atmospheric neutrino data and the LSND results. All these experimental results can be accommodated in a single neutrino oscillation framework only if there are at least three different scales of neutrino mass-squared differences. The simplest case of three independent mass-squared differences requires the existence of a light sterile neutrino, *i.e.* one whose interaction with standard model particles is much weaker than the SM weak interaction, so it does not affect the invisible Z decay width, precisely measured at LEP.

There are six possible four-neutrino schemes that can accomodate all these evidences. They can be divided in two classes: 3+1 and 2+2. In the 3+1 schemes there is a group of three neutrino masses separated from an isolated mass by a gap of the order of 1eV which gives the mass-squared difference responsible for the short-baseline oscillations observed in the LSND experiment. In 2+2 schemes there are two pairs of close masses separated by the LSND gap. 3+1 schemes are disfavoured by experimental data with respect to the 2+2 schemes but they are still marginally allowed.

As discussed in Ref. [5], for any of these four-neutrino schemes, either 2+2 or 3+1, only four mixing angles are relevant in the study of solar neutrino oscillations [1,2,8]. The survival of solar ν_e 's mainly depends on the mixing angle ϑ_{12} , whereas the mixing angles ϑ_{23} and ϑ_{24} determine the relative amount of transitions into sterile ν_s or active ν_a , this last one being a combination of ν_μ and ν_τ controlled by the mixing angle ϑ_{34} . ν_μ and ν_τ cannot be distinguished in solar neutrino experiments, because their matter potential and their interaction in the detectors are equal, due only to NC weak interactions. As a consequence the active/sterile ratio and the survival probability

for solar neutrino oscillations do not depend on the mixing angle ϑ_{34} , and depend on the mixing angles ϑ_{23} ϑ_{24} only through the combination $\cos \vartheta_{23} \cos \vartheta_{24}$. For further details see Ref. [1,2].

In the general case of simultaneous $\nu_e \rightarrow \nu_s$ and $\nu_e \rightarrow \nu_a$ oscillations the corresponding probabilities are given by [1,2]

$$P_{\nu_e \rightarrow \nu_s} = c_{23}^2 c_{24}^2 (1 - P_{\nu_e \rightarrow \nu_e}) , \quad (1)$$

$$P_{\nu_e \rightarrow \nu_a} = (1 - c_{23}^2 c_{24}^2) (1 - P_{\nu_e \rightarrow \nu_e}) . \quad (2)$$

where $P_{\nu_e \rightarrow \nu_e}$ takes the standard two-neutrino oscillation form for Δm_{12}^2 and θ_{12} but computed with the modified matter potential $A \equiv A_{CC} + c_{23}^2 c_{24}^2 A_{NC}$. Thus the analysis of the solar neutrino data in the four-neutrino mixing schemes is equivalent to the two-neutrino analysis but taking into account that the parameter space is now three-dimensional ($\Delta m_{12}^2, \tan^2 \vartheta_{12}, \cos^2 \vartheta_{23} \cos^2 \vartheta_{24}$). We want to stress that, although originally this derivation was performed in the framework of the 2+2 schemes [1,2], it is equally valid for the 3+1 ones [8].

The allowed regions in the three-parameter space for the global combination of observables are shown in Ref. [3]. The global minimum used in the construction of the regions lays in the LMA region and for pure ν_e -active oscillations, $c_{23}^2 c_{24}^2 = 0$. The SMA region is always a valid solution for any value of $c_{23}^2 c_{24}^2$ at 95% CL ($0.11 < c_{23}^2 c_{24}^2 < 0.31$ allowed at 90% CL). On the other hand, the LMA and LOW-QVO solutions disappear for increasing values of the mixing $c_{23}^2 c_{24}^2$ (0.72 and 0.76 at 99% CL, respectively).

4. Expected Rates at SNO in Four-Neutrino Schemes

In this section, we present the predictions for the CC ratio and for the NC/CC ratio in the four-neutrino scenario previously described. This scenario contains as limiting cases the pure ν_e -active and ν_e -sterile neutrino oscillations.

In Figs. 2–4 we show the results for the predicted [CC] ratio and [NC]/[CC] ratio for the different allowed regions (SMA, LMA, LOW-QVO) at 90 and 99 %CL as a function of $c_{23}^2 c_{24}^2$. The general behaviour of the dependence of the pre-

dicted ratios with $c_{23}^2 c_{24}^2$ can be easily understood using the following simplified expressions:

$$[\text{CC}] \sim P_{\nu_e \rightarrow \nu_e}, \quad (3)$$

$$\frac{[\text{NC}]}{[\text{CC}]} \sim \frac{1 - c_{23}^2 c_{24}^2 (1 - P_{\nu_e \rightarrow \nu_e})}{P_{\nu_e \rightarrow \nu_e}}. \quad (4)$$

From Eq. (3), the only dependence of $[\text{CC}]$ on $c_{23}^2 c_{24}^2$ is due to the modification of the matter potential entering in the evolution equation and it is very weak. The dependence of the allowed range of the $[\text{CC}]$ ratio with $c_{23}^2 c_{24}^2$ displayed in the figures arises mainly from the variation of the size of the allowed regions. Alternatively following Eq. (4) we find a stronger linear dependence of $[\text{NC}]/[\text{CC}]$ on $c_{23}^2 c_{24}^2$ with slope $(-1 + P_{\nu_e \rightarrow \nu_e})/P_{\nu_e \rightarrow \nu_e} \sim 1 - 1/[\text{CC}]$ and intercept $1/P_{\nu_e \rightarrow \nu_e} \sim 1/[\text{CC}]$. This simple description is able to reproduce the main features of our numerical calculations as can be seen in the figures.

Figs. 2–4 contain the main quantitative result of our analysis in the four-neutrino mixing scenario. From each of them it is possible to infer the allowed range of the active–sterile admixture, $c_{23}^2 c_{24}^2$, compatible, within the expected uncertainty, with a given SNO measurement of the ratios. Also, comparing the allowed ranges for the different solutions one can study the potential of these measurements as discriminatory among the three presently allowed regions. Of course, both issues are not independent as we have no “a priori” knowledge of which is the right solution and both must be discussed simultaneously. In order to do so we pass to describe and compare in detail the predictions in the different regions.

The results for the SMA solution are shown in Fig. 2.a and 2.b for $[\text{CC}]$ and $[\text{NC}]/[\text{CC}]$ ratios respectively. First we notice that we find a small region allowed at 90 %CL only for a non-vanishing admixture of active and sterile oscillations as mentioned before. In this region $[\text{CC}] \sim 0.65\text{--}0.73$ and $[\text{NC}]/[\text{CC}] \sim 1.3\text{--}1.4$. The predictions at 99% range from $[\text{CC}] \sim 0.4\text{--}0.9$ ($[\text{NC}]/[\text{CC}] \sim 1.1\text{--}2.5$) for pure ν_e –active scenario to to $[\text{CC}] \sim 0.59\text{--}0.85$ ($[\text{NC}]/[\text{CC}] \sim 0.96\text{--}0.98$) for pure ν_e –sterile oscillations. Thus if SNO observes a ratio $[\text{CC}] < 0.58$ the value of $c_{23}^2 c_{24}^2$ can be constrained to be smaller than 1 disfavouring pure ν_e –sterile oscillations. On the contrary a

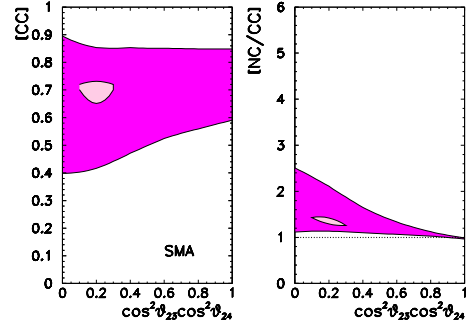


Figure 2. $[\text{CC}]$ and $[\text{NC}]/[\text{CC}]$ predictions at SNO as for the SMA region in the four-neutrino scenario obtained from the global analysis of solar neutrino data at 90 % (lighter) and 99 %CL (darker). The dotted line corresponds to the prediction in the case of no oscillations.

measurement of $[\text{CC}] \gtrsim 0.68$ will immediately hint towards the SMA solution but will not provide any information on the active–sterile admixture. Also, one must notice, that such value, although allowed by the present global statistical analysis at 99 %CL, will imply a strong disagreement with the total rate event rate observed at Super-Kamiokande.

As seen in Fig. 2.b the $[\text{NC}]/[\text{CC}]$ ratio is more sensitive to the active–sterile admixture. To guide the eye, in the figures for the $[\text{NC}]/[\text{CC}]$ ratio we plot a dotted line for the prediction in the case of no oscillation $[\text{NC}]/[\text{CC}] = 1$. For any of the solutions, the allowed range for this ratio shows as general behaviour a decreasing with $c_{23}^2 c_{24}^2$ due to two effects: (i) the allowed regions become smaller and (ii) the prediction decreases when more sterile neutrino is involved in the oscillations as described in Eq. (4). The measurement of higher values of this ratio will favour the four-neutrino scenario with larger component of ν_e –active oscillations. On the other hand a measurement of $[\text{NC}]/[\text{CC}] \sim 1$, will push the oscillation hypothesis towards the pure ν_e –sterile oscillation scenario. This case will be harder to differentiate from the non-oscillation scenario. We find that with the expected sensitivity the parameter $c_{23}^2 c_{24}^2$ is constrained to be above 0.44 at 99% CL and

that the pure ν_e -active oscillations in the SMA region are compatible with $[\text{NC}]/[\text{CC}]=1$ only at $\sim 5\sigma$. The predictions for oscillation param-

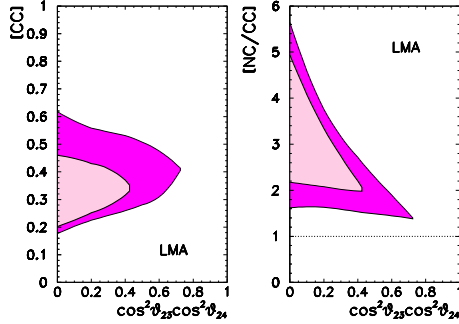


Figure 3. Same as Fig. 2 for the LMA region.

eters in the LMA region are shown in Figs. 3.a and 3.b for $[\text{CC}]$ and $[\text{NC}]/[\text{CC}]$ ratios respectively. The predictions at 99% vary in the range $[\text{CC}]\sim 0.18\text{--}0.62$ and $[\text{NC}]/[\text{CC}]\sim 1.4\text{--}5.6$. The first thing we notice by comparing Fig. 3.a with Fig. 2.a and Fig. 4.a is that the most discriminatory scenario for the $[\text{CC}]$ rate results if SNO finds a small value $[\text{CC}]\sim 0.25$. This would significantly hint towards the LMA solution to the solar neutrino problem and towards ν_e -active oscillation scenario. First, it is well separated from the predictions for the SMA and LOW regions. Second, it will include as a bonus a small but measurable day-night asymmetry. And third it will constrain the $c_{23}^2 c_{24}^2$ to a small value (~ 0.2). On the contrary the less discriminatory scenario will be a measurement $0.4 < [\text{CC}] < 0.6$ where the prediction would be compatible with both SMA and LOW-QVO solutions and no improvement on our knowledge of the four-neutrino schemes is possible. The $[\text{NC}]/[\text{CC}]$ ratio can definitively improve the discrimination between the different scenarios provided its measurement lays in the upper range. For instance a measurement of $[\text{NC}]/[\text{CC}]\sim 4$ (± 0.7 at 5σ) will be conclusive for selecting LMA as the solution to the SNP and will imply an upper bound on $c_{23}^2 c_{24}^2 < 0.3$. The predictions for the LOW-QVO region lay between the ones for SMA

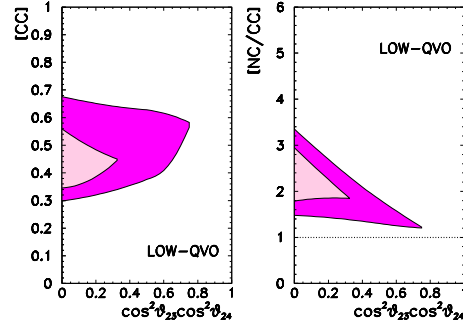


Figure 4. Same as Fig. 2 for the LOW region.

and LMA as displayed in Fig. 4 and therefore they are more difficult to discriminate. The predictions at 99% vary in the range $[\text{CC}]\sim 0.3\text{--}0.68$ and $[\text{NC}]/[\text{CC}]\sim 1.2\text{--}3.4$. As a consequence we see that a low $[\text{CC}]$ ratio but still within the 99% CL range allowed for this region, $0.3 < [\text{CC}] < 0.4$, will constrain significantly the $c_{23}^2 c_{24}^2$ parameter compatible with this solution but it will not be distinguishable from the LMA solution unless the measured $[\text{CC}] < 0.3$. As mentioned above, the $[\text{NC}]/[\text{CC}]$ ratio will be able to differentiate the LMA and LOW-QVO solutions if not in the range $[1.5, 3]$. One should also notice that for the upper part of this range a positive measurement of the day-night asymmetry and the zenith dependence will point towards the higher Δm^2 of the LOW region as the solution.

This work was supported by grants DGICYT-PB98-0693 and PB97-1261, GV99-3-1-01, EU network ERBFMRXCT960090 and ESF network 86.

REFERENCES

1. D. Dooling *et al.*, Phys. Rev. **D61**, 073011 (2000).
2. C. Giunti *et al.*, Phys. Rev. **D62**, 013005 (2000).
3. M. C. Gonzalez-Garcia, these proceedings.
4. J. N. Bahcall *et al.*, astro-ph/0010346.
5. Gonzalez-Garcia *et al.*, hep-ph/0011245.
6. S. Nakamura *et al.*, nucl-th/0009012.
7. J. N. Bahcall *et al.*, Phys. Rev. **D62** 093004 (2000).

8. C. Giunti and M. Laveder, hep-ph/0010009.